Cell Biology of Mating in *Candida albicans*

Shawn R. Lockhart, Karla J. Daniels, Rui Zhao,
Deborah Wessels, and David R. Soll*

*Department of Biological Sciences, The University of Iowa,
Iowa City, Iowa 52242*

It was recently demonstrated that strains homozygous for either of the mating type-like loci *MTL*a and *MTL*α of *Candida albicans* undergo white-opaque switching and that expression of the opaque-phase phenotype greatly enhances mating between strains. Exploiting the latter property to obtain high-frequency mating, we have characterized the cell biology of the mating process of *C. albicans*. Employing continuous videomicroscopy, computer-assisted three-dimensional reconstruction of living cells, and fluorescence microscopy, we have monitored the mating-associated processes of conjugation, tube formation, fusion, budding, septum formation, and daughter cell development and the spatial and temporal dynamics of nuclear migration and division. From these observations, a model for the stages in *C. albicans* mating is formulated. The stages include shmooing, chemotropism of conjugation tubes, fusion of tubes and nuclear association, vacuole expansion and nuclear separation in the conjugation bridge, asynchronous nuclear division in the zygote, bud growth, nuclear migration into the daughter cell, septation, and daughter cell budding. Since there was no cytological indication of karyogamy, genetic experiments were performed to assess marker segregation. Recombination was not observed, suggesting that mating takes place in the absence of karyogamy between naturally occurring, homozygous a and α strains. This study provides the first description of the cell biology of the mating process of *C. albicans*.

Candida albicans is a diploid organism that, until quite recently, was believed to have no sexual cycle. However, in 1999 Hull and Johnson (13) demonstrated that *C. albicans* strain CAI4 contained *MTL*a*1* on one chromosome and *MTL*α*1* and *MTL*α*2* on the homolog. Soon after, fusion was genetically demonstrated to occur between *MTL*a and *MTL*α strains (a/− and α/−, respectively) in vivo (14) and in vitro (20). Recently, Miller and Johnson (21) demonstrated that the homozygous *MTL*a and *MTL*α strains engineered from strain CAI4 underwent white-opaque switching and that when both strains were in the opaque phase, mating occurred 10^6 times more efficiently than when one or both strains were in the white phase. Lockhart et al. (17) subsequently demonstrated that approximately 3% of 220 clinical isolates of *C. albicans* representing the major clades worldwide were homozygous for the mating type locus (i.e., either *MTL*a or *MTL*α), that all tested clinical strains that underwent white-opaque switching were homozygous for *MTL*, that most clinical strains that were homozygous for *MTL* underwent the white-opaque transition, and that heterozygotes did not undergo white-opaque switching. Together, these recent results demonstrate for the first time that the mating type locus regulates switching and that switching facilitates mating.

To visualize the mating process of *C. albicans*, we took advantage of the recent discovery that mating is facilitated by the opaque-phase phenotype (21). Using information obtained from videomicroscopy, computer-assisted dynamic three-dimensional (3D) reconstruction techniques (31, 35, 36), and fluorescence microscopy, we describe here for the first time the cell biology of mating-associated fusion and zygote formation in *C. albicans*.

MATERIALS AND METHODS

Strain maintenance and growth. All strains used in this study (Table 1) were maintained in 20% glycerol at −80°C. For experimental purposes, cells were plated on agar containing modified Lee's medium, an amino acid-containing defined medium supplemented with zinc and arginine (2). The agar also contained, per ml, 5 µg of phloxine B, which differentially stains opaque-phase cells and colonies red (1). Opaque-phase cells were obtained from red colonies, and the unique opaque-phase cell phenotype (1, 30, 33) was verified microscopically.

Mixing of *MTL*a and *MTL*α cells. Cells from 5- to 7-day colonies were inoculated into modified Lee's medium and grown for 12 h at 25°C in suspension. Cells were then pelleted and resuspended in fresh modified Lee's medium. Approximately 10^7 cells from each of two strains were mixed in a standard manner in a final volume of 1 ml of medium in a plastic 15-ml Falcon tube, and the tube was incubated at 25°C at a rotation speed of 250 rpm in a water bath shaker. In some cases, mixed cultures were then transferred to agar containing sporulation medium (1% [wt/vol] potassium acetate, 2% agar) (29).

PCR and Southern blot analyses. DNA was prepared (28) and resuspended in water for PCR. One nanogram of total genomic DNA was used as a template with the primer set 5′-CATACCCAAACTCTTTATTTGGG-3′ and 5′-CACCC ACCTTCAACCTCCTCGTTTTTTCC-3′ for the amplification of *MTL*a*1* and with the primer set 5′-CACATCTGGAGGCACTCTTTG-3′ and 5′-GGTCTT TTTGCAGATACGGA-3′ for the amplification of *MTL*α*2* by using *Taq* DNA polymerase as recommended by the manufacturer (Invitrogen, Carlsbad, Calif.). After an initial denaturation step of 10 min at 95°C, the reaction conditions consisted of 40 cycles of the following program: 94°C for 1 min, 42°C for 2 min, and 68°C for 3 min. The final elongation step was 10 min at 68°C.

Continuous videorecordings and 3D-DIAS reconstruction of fusion. After 2 h, cells from mixed cultures were dispersed on the glass wall of a Dvorak-Stotler chamber (Lucas-Highland Inc., Chantilly, Va.) and positioned on a Zeiss ICM405 microscope equipped with differential interference contrast (DIC) optics. For two-dimensional time-lapse sequences of fusion, cells were continuously videorecorded onto digital videotape at a ×630 magnification. Images were selected by using Adobe Premiere software (Adobe Systems Inc., San Jose, Calif.). For 3D-DIAS reconstructions of fusion, two cells that appeared to be

TABLE 1. Strains used in this study

Strain	Origin	*MTL* genotype	Clade[a]	Reference
WO-1	Bloodstream	α	II	30
19F	Vagina	α	I	18
P78048	Mouth	α	I	24
L26	Vagina	**a**	I	17
12C	Mouth	**a**	I	18
P37005	Mouth	**a**	I	17
P75063	Bloodstream	**a**	SA	24
3153A	Lab	**a**/α	I	

[a] By using the Ca3 probe and Southern blot hybridization, *C. albicans* has been separated into five major clades: group I, group II, group III, group SA, and group E (3, 17, 23, 24).

extending incipient tubes toward each other were selected from among clumps of cells. The methods for collecting optical sections, outlining the perimeters of cells, and completing 3D reconstruction have been previously described in detail (12, 31, 35, 36). In brief, 60 optical sections were collected through DIC optics in a 2-s period and this procedure was repeated every 5 s. The two cells were color-coded red and yellow prior to fusion, and the zygote was color-coded orange after fusion.

Isolation of daughter cells from zygotes. Mating mixtures were grown in suspension in modified Lee's medium. Cells were dispersed on yeast extract-peptone-dextrose (YPD) agar, zygotes were identified, and single daughter cells were picked by using a micromanipulator. Daughter cells were individually plated on YPD agar over a grid so that the resulting colonies could be relocated. After 48 h, cells from the resulting colonies were clonally plated on YPD agar plates.

Fluorescent staining. To stain nuclei, cells were washed three times in double-distilled water and then incubated in a solution containing 1 μg of Hoechst 33342 (Molecular Probes, Eugene, Oreg.) per ml for 1 h at room temperature. In triple-labeling experiments, live cells from one mating type were incubated for 1 h in 10 μg of rhodamine-conjugated concanavalin A (rhodamine-ConA; Vector Laboratories, Burlingame, Calif.) ml^{-1} and those from the other mating type were incubated in 10 μg of fluorescein isothiocyanate-conjugated ConA (FITC-ConA; Vector Laboratories) ml^{-1}. The cells were washed free of unbound lectin and mixed as previously described. After mating, cells were stained with 5 μM calcofluor white M2R (Molecular Probes) for 15 min at room temperature. Wet mounts were prepared on poly-L-lycine-coated microscope slides. Fluorescently labeled cells were visualized with a Zeiss Axioplan II microscope with a mercury lamp. Transmitted light images were gathered by using either DIC or phase-contrast optics. Images were recorded with either a Nikon Cool Pix 990 or a Zeiss AxioCam digital camera. Multichannel images were grabbed and superimposed by using Zeiss Axio-Vision software. Image processing was performed with Adobe Photoshop software.

RESULTS

MTL* genotypes and switch phenotypes.** Four homozygous *MTLa** strains (L26, 12C, P37005, and P75063), three homozygous *MTL*α strains (WO-1, 19F, and P78048), and one heterozygous *MTL***a**/*MTL*α strain (3153A) were used in crosses (Table 1). The *MTL* genotype of each strain was verified by PCR analysis (17). Each strain was also characterized for white-opaque switching. The four *MTL***a** and three *MTL*α strains all switched reversibly between white and opaque at frequencies of approximately 10^{-3}. As previously described (1, 30, 33), white-phase cells were round and formed round daughter cells while opaque-phase cells were elongate, bean shaped, and larger than white-phase cells and formed elongate daughter cells. The heterozygous strain 3153A did not undergo the white-opaque transition, remaining fixed in the white-phase phenotype.

Tube formation in mixed cultures of homozygous *MTL*a**

cells and homozygous *MTL*α cells. When opaque-phase cells from single homozygous *MTL***a** and *MTL*α strains were grown in suspension cultures at 25°C in modified Lee's medium, they continued to multiply exclusively with the opaque budding phenotype (Fig. 1A and B, respectively). When mixtures of opaque-phase cells from two *MTL***a** strains or from two *MTL*α strains were grown in suspension in modified Lee's medium, cells also continued to multiply exclusively with the opaque budding phenotype (Fig. 1C and D, respectively). Even after 48 h of incubation, no tubes were seen in opaque-phase cultures. However, when mixtures of opaque-phase cells from an *MTL***a** strain and an *MTL*α strain (50% *MTL***a** cells, 50% *MTL*α cells) were grown in suspension in modified Lee's medium, cells stopped multiplying and after 1.5 h formed evaginations that elongated into tubes (Fig. 1E and F). Evaginations formed from the sides as well as the ends of the elongate opaque-phase cells. As is the case in the formation of hyphae (32), the junctions between mother cells and evaginations were not constricted (Fig. 1G through J). However, in contrast to what occurs in hypha formation, there was no indication of septation or compartmentalization along the tubes, even when tubes reached lengths greater than the diameters of the mother cells (Fig. 1K and L). In the process of hypha formation, the first septum forms along the tube on average 2 μm from the junction of the mother cell and the tube, the approximate diameter of the mother cell (22, 32).

Tubes that formed in crosses of homozygous *MTL***a** cells and homozygous *MTL*α cells grew to lengths up to six or seven times the diameters of their mother cells. Mother cells frequently became round during tube growth. In some cases, tube growth terminated in the formation of an apical bud in a fashion similar to that recently reported for the unique tubes formed by *Candida glabrata* (15). Together, these results demonstrate that only mixtures of *MTL***a** and *MTL*α opaque-phase cells form conjugation tubes, that these conjugation tubes are architecturally different from hyphae, and that the majority of cells in a 50:50 mixture of *MTL***a** and *MTL*α opaque-phase cells, and hence with cells of both mating types, form tubes.

Fusion in mixed cultures of homozygous *MTL*a** cells and homozygous *MTL*α cells.** When mixed cultures of homozygous *MTL***a** cells and homozygous *MTL*α cells in the opaque phase (50% *MTL***a** cells, 50% *MTL*α cells) were incubated in suspension for more than 2 h in Lee's medium, the cells formed large clumps within which they underwent fusion. Fusion occurred at a very low frequency in water and 1 M sorbitol and did not occur at all in *Saccharomyces cerevisiae* sporulation medium (29). Clumping was facilitated by adhesion between tubes. In Fig. 2, images from 5-min intervals of a fusion event videorecorded through DIC optics are shown. In this case, *MTL***a** (P37005) cells and *MTL*α (WO-1) cells were mixed in Lee's medium, incubated for 2 h in suspension, and then dispersed on a glass slide and immediately videorecorded. In this particular example, two cells made contact and then sent out protrusions at the point of contact. The protrusions elongated and at 65 min fused at the point of contact. The fused projections expanded between 65 and 95 min into a conjugation bridge, which continued to elongate. Focusing through the z axis revealed that no septum had formed between the two cells and that the cytoplasms were contiguous. Five additional fusions were monitored in a similar fashion. In all cases, the evagina-
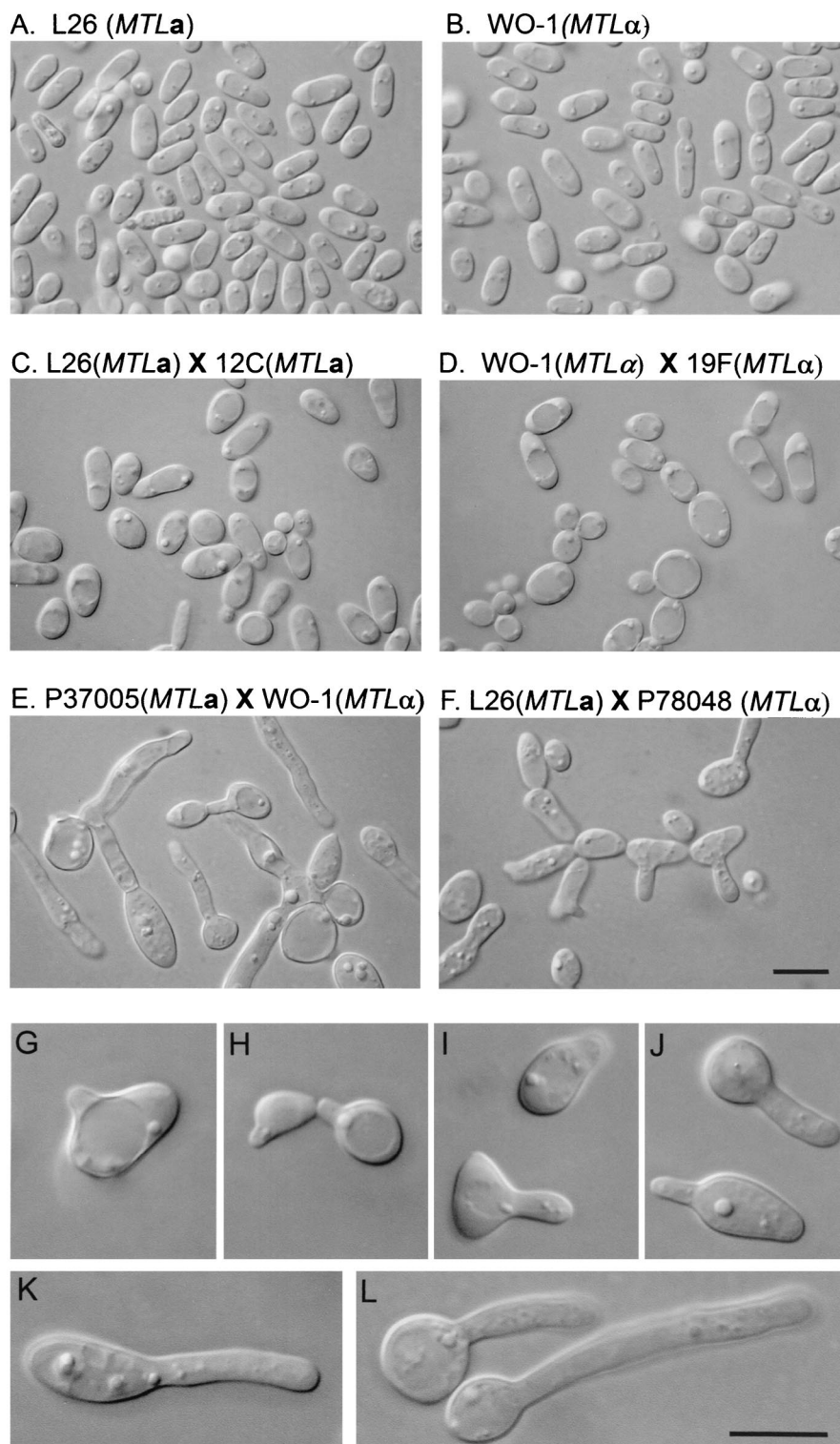
FIG. 1. Tube formation occurs exclusively in mixtures of *MTL***a** and *MTL*α cells. Cells were imaged through DIC optics. (A) Homogeneous culture of strain L26 (*MTL***a**) opaque-phase cells; (B) homogeneous culture of WO-1 (*MTL*α) opaque-phase cells; (C) mixture of L26 (*MTL***a**) and 12C (*MTL***a**) opaque-phase cells (50:50); (D) mixture of WO-1 (*MTL*α) and 19F (*MTL*α) opaque-phase cells (50:50); (E) mixture of P37005 (*MTL***a**) and WO-1 (*MTL*α) opaque-phase cells (50:50); (F) mixture of L26 (*MTL***a**) and P78048 (*MTL*α) opaque-phase cells; (G to J) higher-magnification images of incipient tube formation in mixtures of *MTL***a** and *MTL*α opaque-phase cells; (K and L) tube formation in mixtures of *MTL***a** and *MTL*α opaque-phase cells. Scale bars, 5 μm.
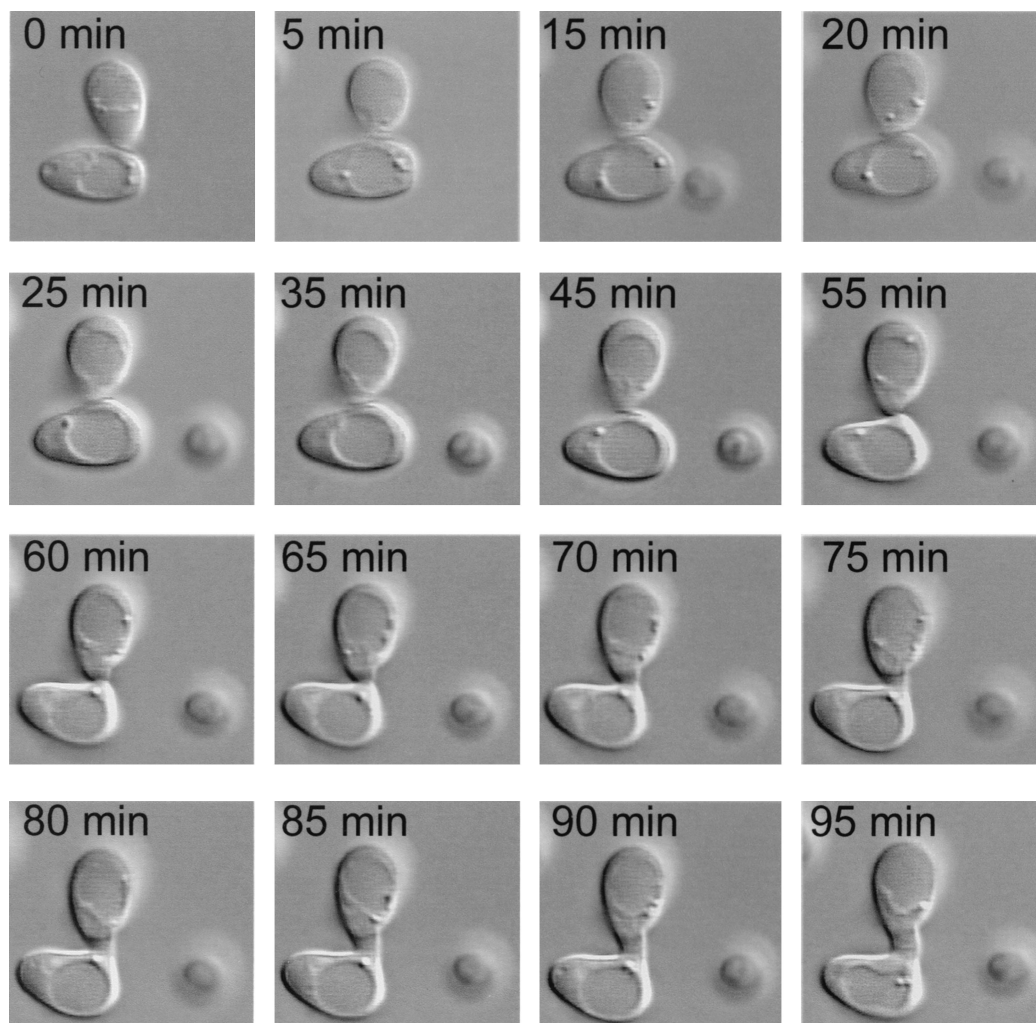
FIG. 2. Sequence of video images of two cells undergoing fusion in a mixture of *MTL***a** (P37005) and *MTL*α (WO-1) opaque-phase cells. Cells were imaged through DIC optics. Fusion occurred at 65 min.

tions from opposing cells extended toward each other in a manner that suggested a chemotrophic mechanism. The accuracy of the fusion process is evident in 3D-DIAS reconstructions of one such fusion (Fig. 3). In this particular example, the two cells (cell 1 and cell 2) were in a clump of seven cells. Cell 1 is color-coded red, and cell 2 is color-coded green. Cell 1 was above the substratum (grid) since it was atop three other cells that were not reconstructed in 3D and are, therefore, invisible in Fig. 3. At the start of the time series (0 min), each of the two cells had already extended a projection toward that of the other cell (Fig. 3). The accuracy of tube extension was quite remarkable. Between 18 and 20 min, the ends of the two extensions, which had become perfectly juxtaposed, made contact and fused (Fig. 3). The zygote is color-coded orange.

Proof that only cells of opposite mating types fuse in mixed cultures. To prove that only cells of opposite mating types fuse in mixed cultures, before being mixed, cells from strain P37005 (*MTL***a**) were stained with the vital dye FITC-ConA, which stained cells green (Fig. 4A), and cells from strain WO-1 (*MTL*α) were stained with the vital dye rhodamine-ConA, which stained cells red (Fig. 4B). Four hours after being mixed,

cells were fixed and further stained with calcofluor, which stained entire cell walls blue (Fig. 4C). If fusions occurred only between cells of opposite mating types, then fusants would be made up exclusively of one cell body stained green and another cell body stained red. No fusants would include green-green or red-red combinations. In Fig. 4, three examples of fusants are presented. In each fusion, one cell stained green (*MTL***a**) and one cell stained red (*MTL*α) (Fig. 4F, I, and L). In each case, new cell wall growth and the conjugation tube were devoid of green or red stain (Fig. 4F, I, and L), staining exclusively blue with calcofluor (Fig. 4E, H, and K). Of 100 zygotes analyzed by fluorescence microscopy, 100% included one green and one red parent cell; 0% included two green or two red parent cells. These results demonstrate that only opaque-phase cells of opposite mating types fuse in a mixed culture.

To demonstrate that this conclusion can be generalized, opaque-phase cells of 12 different combinations of *MTL***a** and *MTL*α strains were mixed and assayed for fusion. In all cases, fusions (zygotes) were observed (Table 2). In five different crosses in which opaque-phase cells from two different *MTL***a** strains were mixed and in three different crosses in which
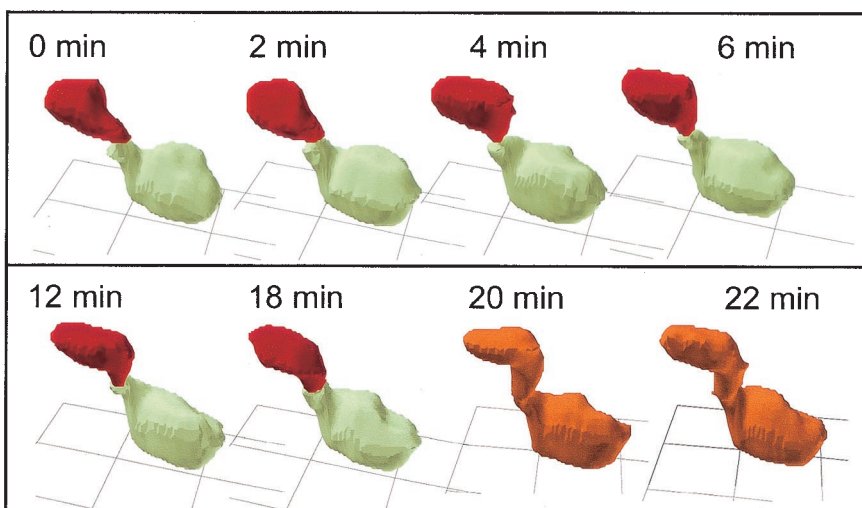
A. 5 deg
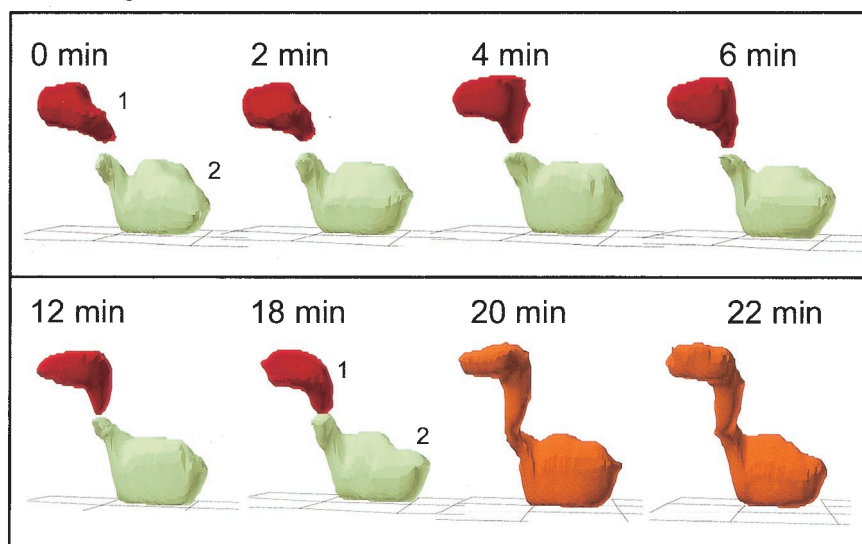
B. 35 deg

FIG. 3. 3D-DIAS reconstruction of fusion between two cells in a clump of cells from a mixture of *MTL***a** (P37005) and *MTL*α (WO-1) cells. The red cell (cell 1) was high up in the clump of cells while the green cell (cell 2) was at the bottom of the clump. Nonfusing cells in the clump were not reconstructed. After fusion occurred, the zygote was color-coded orange. Reconstructed cells are viewed from angles of 5° (A) and 35° (B) relative to the substratum (grid). deg, degree.

opaque cells from two different *MTL*α strains were mixed, no fusions were observed (Table 2). In three crosses in which opaque-phase cells from three different *MTL***a** strains were mixed with *MTL***a**/*MTL*α cells and in three crosses in which opaque cells from three different *MTL*α strains were mixed with *MTL***a**/*MTL*α cells, no fusions were observed (Table 2). Finally, when either or both strains were white in an *MTL***a** × *MTL*α cross, no fusions were observed (Table 2). These results provide cytological evidence that the genesis of zygotes occurs only between opaque-phase cells of a homozygous *MTL***a** strain and a homozygous *MTL*α strain.

Fusion results in a single daughter cell. After fusion, the conjugation bridge swelled and from this tube a bud formed

(Fig. 5). Calcofluor staining revealed first a faint septum at the interface between the daughter cell and the conjugation bridge (Fig. 5A). Daughter cells could be either round, like white-phase cells, or elongate, like opaque-phase cells, but the majority were elongate. However, secondary daughter cells that formed off the original daughter cell were all round (see Fig. 7J, L, N, and O), suggesting a reversion to the white phase. When daughter cells matured, septa stained more intensely (Fig. 5B through D). No septa formed at the junctions of the conjugation tubes and either of the parent cells (Fig. 5A through D). Zygotes, therefore, possessed only one septum, positioned at the junction of the daughter cell and the tube. This landmark could be used to distinguish the daughter cell
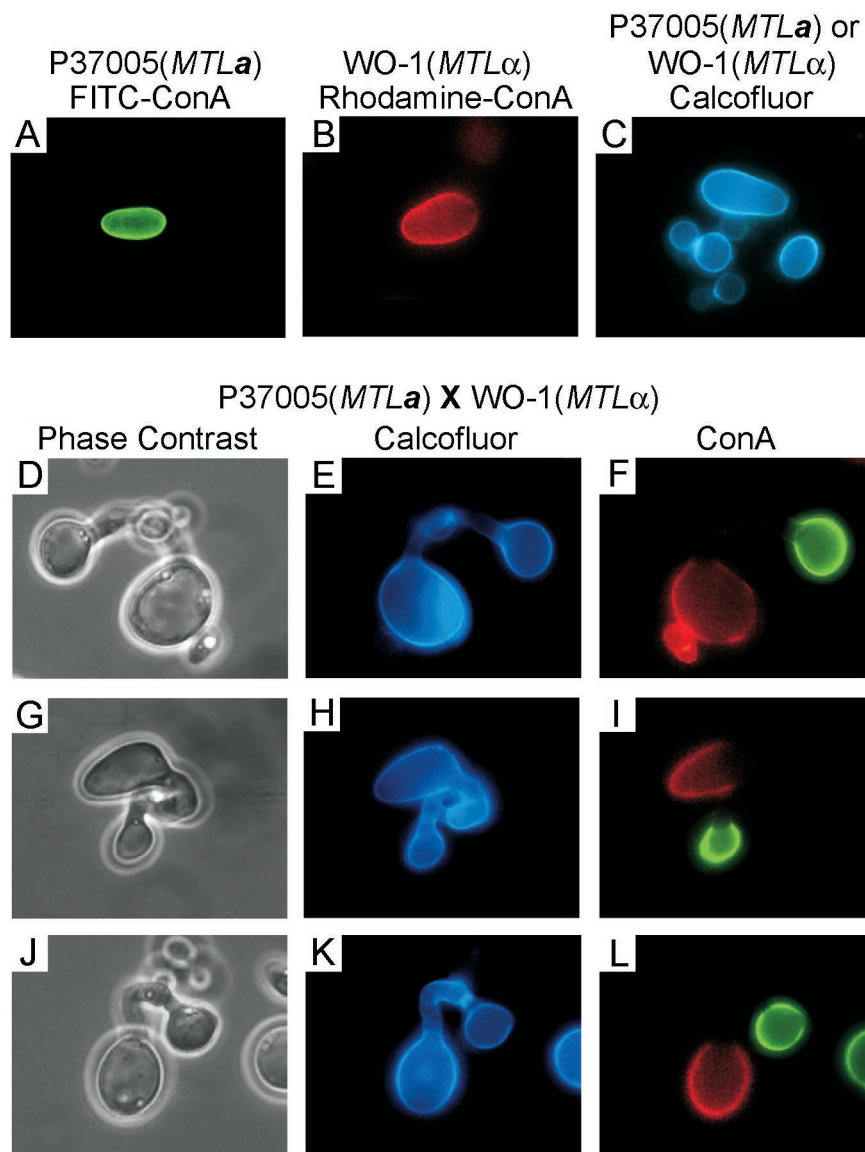
P37005(*MTL***a**)
FITC-ConA

WO-1(*MTL*α)
Rhodamine-ConA

P37005(*MTL***a**) or
WO-1(*MTL*α)
Calcofluor

P37005(*MTL***a**) **X** WO-1(*MTL*α)

Phase Contrast   Calcofluor   ConA

FIG. 4. Demonstration by ConA staining that only *MTL***a** and *MTL*α cells fuse. *MTL***a** cells (strain P37005) were vitally stained with FITC-ConA, *MTL*α cells were vitally stained with rhodamine-ConA, and the cells were mixed. Fusants were subsequently stained with calcofluor. (A) Unfused *MTL***a** cell stained with FITC-ConA; (B) Unfused *MTL*α cell stained with rhodamine-ConA; (C) unfused cells stained with calcofluor; (D, G, and J) phase-contrast images of zygotes; (E, H, and K) fluorescent images of calcoflour-stained zygotes; (F, I, and L) fluorescent images of rhodamine-ConA–FITC-ConA-labeled zygotes. Of 100 zygotes, 100% were combinations of green-red, 0% were green-green, and 0% were red-red. Scale bar, 5 μm.

from the two parental cells in a fusion complex. With a fiber-optic needle and micromanipulation, the mature daughter cell could easily be separated from the conjugation bridge, but the two parental cells of the zygote were not viable following separation from the bridge.

Tube formation and nuclear behavior. Cells formed tubes only in mixed cultures of homozygous *MTL***a** and homozygous *MTL*α opaque-phase cells (Fig. 1). When the proportion of one of the mating types was skewed (e.g., 80% *MTL***a** cells and 20% *MTL*α cells or 20% *MTL***a** cells and 80% *MTL*α cells), the proportion of cells with long tubes increased while the proportion of fusions (zygotes) decreased (data not shown). This observation suggested that tubes grew longer and the number

of fusions decreased when the chance of finding a cell of the opposite mating type decreased. These mating-induced tubes differed from traditional hyphae by the absence of septation and compartmentalization (Fig. 1E, F, J, K, and L). These tubes also differed from traditional hyphae in the behavior of the nuclei. In traditional hyphae, nuclei usually migrate to the junctions of the mother cells and the tubes, where they divide when the hyphae attain a length equal to or greater than the diameters of the mother cells (34). On occasion, nuclei will migrate into the tubes and divide midway down the tubes. In the conjugation tubes formed in mixed cultures of homozygous *MTL***a** cells and homozygous *MTL*α cells, single-cell nuclei exited the mother cells and migrated to the apical ends of the

TABLE 2. Demonstration that only opaque-phase cells of opposite mating types undergo fusion[a]

Mating types	Strains	Cell types	Fusion[b]
*MTL*α × *MTL***a**	WO-1 × L26	Opaque × opaque	+
*MTL*α × *MTL***a**	WO-1 × 12C	Opaque × opaque	+
*MTL*α × *MTL***a**	WO-1 × P37005	Opaque × opaque	+
*MTL*α × *MTL***a**	WO-1 × P75063	Opaque × opaque	+
*MTL*α × *MTL***a**	19F × L26	Opaque × opaque	+
*MTL*α × *MTL***a**	19F × 12C	Opaque × opaque	+
*MTL*α × *MTL***a**	19F × P37005	Opaque × opaque	+
*MTL*α × *MTL***a**	19F × P75063	Opaque × opaque	+
*MTL*α × *MTL***a**	P78048 × L26	Opaque × opaque	+
*MTL*α × *MTL***a**	P78048 × 12C	Opaque × opaque	+
*MTL*α × *MTL***a**	P78048 × P37005	Opaque × opaque	+
*MTL*α × *MTL***a**	P78048 × P75063	Opaque × opaque	+
*MTL*α × *MTL*α	WO-1 × 19F	Opaque × opaque	−
*MTL*α × *MTL*α	WO-1 × P78048	Opaque × opaque	−
*MTL*α × *MTL*α	19F × P78048	Opaque × opaque	−
*MTL***a** × *MTL***a**	L26 × 12C	Opaque × opaque	−
*MTL***a** × *MTL***a**	L26 × P37005	Opaque × opaque	−
*MTL***a** × *MTL***a**	L26 × P75063	Opaque × opaque	−
*MTL***a** × *MTL***a**	12C × P37005	Opaque × opaque	−
*MTL***a** × *MTL***a**	12C × P75063	Opaque × opaque	−
*MTL***a** × *MTL***a**/α	L26 × 3153A	Opaque × white	−
*MTL***a** × *MTL***a**/α	P37005 × 3153A	Opaque × white	−
*MTL***a** × *MTL***a**/α	12C × 3153A	Opaque × white	−
*MTL*α × *MTL***a**/α	WO-1 × 3153A	Opaque × white	−
*MTL*α × *MTL***a**/α	19F × 3153A	Opaque × white	−
*MTL*α × *MTL***a**/α	P78048 × 3153A	Opaque × white	−
*MTL*α × *MTL***a**	WO-1 × L26	Opaque × white	−
*MTL*α × *MTL***a**	19F × L26	White × opaque	−
*MTL*α × *MTL***a**	19F × 12C	White × opaque	−
*MTL*α × *MTL*α	19F × WO-1	White × opaque	−

[a] In this case, fusion in cultures was assessed microscopically 24 and 96 h after cells were mixed.
[b] Mixed cultures were grown for at least 4 days and then analyzed microscopically for fusions. For each culture, 20 fields of cells comparable to those in Fig. 1A through D were scrutinized. +, fusion occurred; −, no fusion occurred.

tubes without dividing (Fig. 6A to C). In cases in which a bud formed at the apex of the tube, the nucleus divided at the tube-bud junction (Fig. 6D). One daughter nucleus entered the apical bud, and the other nucleus migrated back through the tube (Fig. 6E) to the mother cell (Fig. 6F). A septum then formed at the tube-daughter cell junction (Fig. 6F).

Nuclear behavior in the mating process. Preparations of mixed cultures of homozygous *MTL***a** cells and homozygous *MTL*α cells in modified Lee's medium were stained with the nuclear dye Hoechst 33342, and nuclear behavior was interpreted by correlating nuclear staining patterns with the stages of zygote development and daughter cell growth. After evagination, homozygous *MTL***a** cells and homozygous *MTL*α cells extended tubes toward each other until the tips met. Close to the time the tips met, but prior to fusion, the nuclei of the mating cells relocated to the ends of the conjugation tubes (Fig. 7A). Immediately after fusion, the two nuclei localized next to one another at the fusion site along the conjugation bridge (Fig. 7B and C). As the conjugation bridge swelled, the nuclei returned to the junctions of the tube and the parent cell bodies (Fig. 7D to F). The separation of the nuclei correlated with the expansion of a vacuole in the conjugation bridge (Fig. 7D to F). Close to the time of bud formation along the tube,

the two nuclei divided asynchronously so that zygotes contained three to four nuclei on average, one in the swelled tube and two to three associated with the parent cell bodies (Fig. 7G to I). As a daughter cell matured, one nucleus in the majority of cases and two nuclei in the minority of cases migrated into the daughter cell (Fig. 7J through O). After daughter cell maturation, the original fusion complex, consisting of the *MTL***a** and *MTL*α parent cell bodies and the conjugation bridge, contained two (Fig. 7J, K, N, and O) or more (Fig. 7L and M) nuclei. After daughter cells matured, they formed apical buds, which grew into new daughter cells that in turn budded apically (Fig. 7N and O). Each of these secondary daughter cells became nucleated during maturation (Fig. 7O). This interpreted sequence of stages is diagrammed in Fig. 8.

Several caveats to the interpreted scheme must be noted. First, there was no indication of nuclear fusion in the conjugation tubes—i.e., no zygotes which contained only one nucleus midway along the tube soon after fusion were observed. This finding, however, does not rule out the possibility of rapid nuclear fusion and subsequent nuclear division. Second, we could not discern whether each nucleus returned to its original parent cell. Likewise, we could not discriminate which of the two nuclei first divided and, hence, the origin of the nucleus
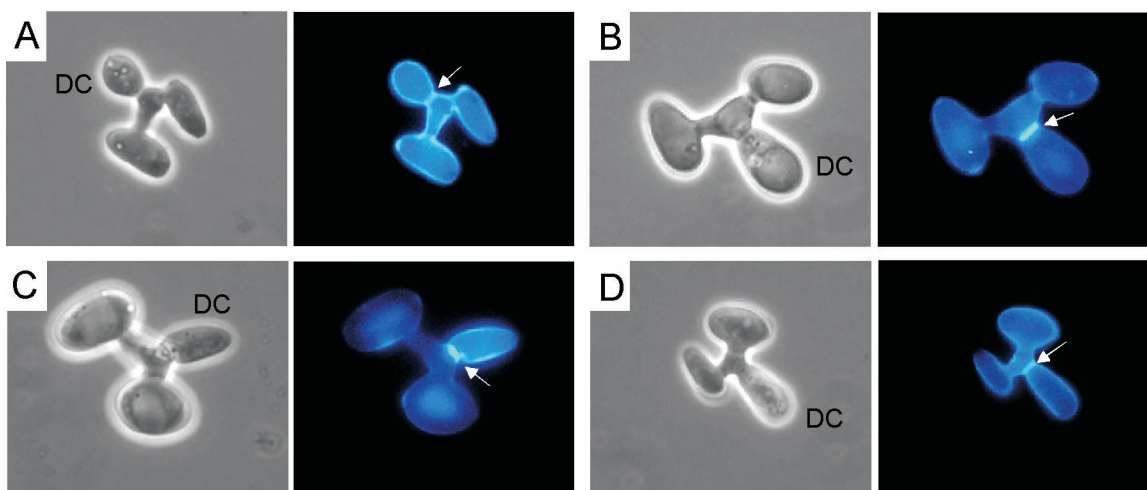
FIG. 5. Daughter cell development and septum formation in *C. albicans* zygotes. Zygotes formed by *MTL***a** and *MTL*α crosses were stained with calcofluor to visualize septa. Each of the four examples (A through D) includes a phase-contrast image and a fluorescent image. Arrows point to septa. DC, daughter cell. Scale bar, 5 μm.

that entered the daughter cell. Third, in daughter cells containing two nuclei, we could not discriminate between the migration of two nuclei into the daughter cell and the migration of one nucleus followed by nuclear division. In some cases, we observed two nuclei through several daughter cell generations. In one colony generated from a binucleate daughter cell, one-third of the daughter cells were still binucleate after at least eight generations.

Mixing of markers from mating partners. Since *C. albicans* is diploid, karyogamy would generate a tetraploid, which may be reduced to a diploid through a reduction division, although meiosis has not been reported for this species. To test for possible nuclear fusion, meiosis, and recombination, strain WO-1 (*MTL*α) was mated with strain P37005 (*MTL***a**) and the inheritance of three markers was analyzed in the progeny of the daughter cell formed from the conjugation bridge. While WO-1 exhibited one *NIK1* band (*NIK1*-1) on a Southern blot, P37005 exhibited two (*NIK1*-1 and *NIK1*-2), and while WO-1 exhibited two *URA3* bands on a Southern blot (*URA3*-1 and *URA3*-2), P37005 exhibited one (*URA3*-1) (Fig. 9; Table 3). *URA3* resides on chromosome 3, *NIK1* resides on chromosome 7, and *MTL* resides on chromosome 5 (Candida Genome Database).

Six mature daughter cells from WO-1 × P37005 zygotes were individually isolated on a YPD agar plate by using a glass needle attached to a micromanipulator. After growth, progeny from each were in turn clonally plated, and 12 were picked for analysis. Of the six fusion daughter cells analyzed, three produced only *MTL***a** progeny, suggesting that only one *MTL***a** nucleus entered each of these daughter cells; two produced only *MTL*α progeny, suggesting that only one *MTL*α nucleus entered each of these daughter cells; and one produced a mixture of three *MTL***a** and nine *MTL*α progeny, suggesting that one *MTL***a** and one *MTL*α nucleus entered this daughter cell (Fig. 9; Table 3). In all cases, *MTL***a** progeny exhibited two *NIK1* bands and one *URA3* band (*URA3*-1), the patterns of the original *MTL***a** parent strain, and *MTL*α progeny exhibited one *NIK1* band (*NIK1*-1) and two *URA3* bands, the patterns of the

original *MTL*α parent strain (Table 3; Fig. 9). This was true for the nine *MTL*α and three *MTL***a** progeny obtained from the single daughter cell 4-5 (Table 3). These results demonstrate that although mating occurred in each case, nuclear fusion did not. These molecular results are consistent with the absence of cytological evidence of nuclear fusion in zygotes (Fig. 7).

Sporulation medium does not induce karyogamy. In *S. cerevisiae*, rich medium supports mating but not meiosis (4). Transfer to sporulation medium supports meiosis. To test whether karyogamy and meiosis occurred in sporulation me-
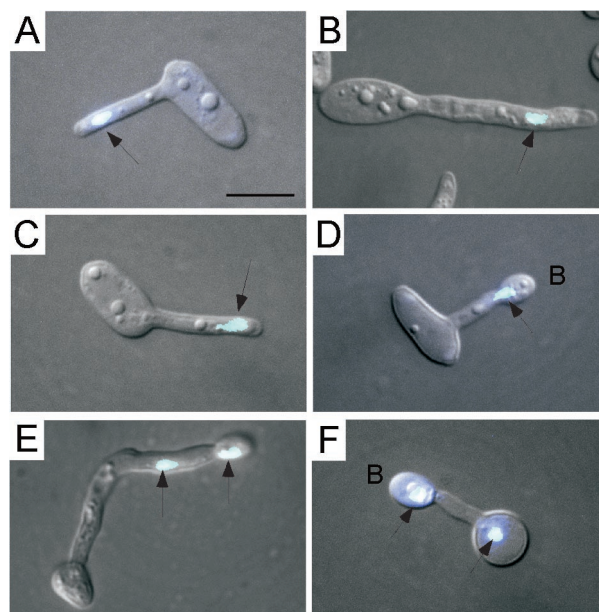

FIG. 6. Nuclear distribution in tubes formed by cells in mixed *MTL***a** and *MTL*α cultures. Nuclei were stained with Hoechst 33342. Fluorescent images of nuclei (blue) are superimposed on phase-contrast images. Arrows point to nuclei. B, terminal bud that forms at the tube apex. Scale bar, 5 μm.

Just prior to fusion
(2 nuclei)

Just after fusion
(2 nuclei)

After fusion - tube expansion
(2 nuclei)

After fusion- daughter cell growth (pre-septum)
(3 nuclei)

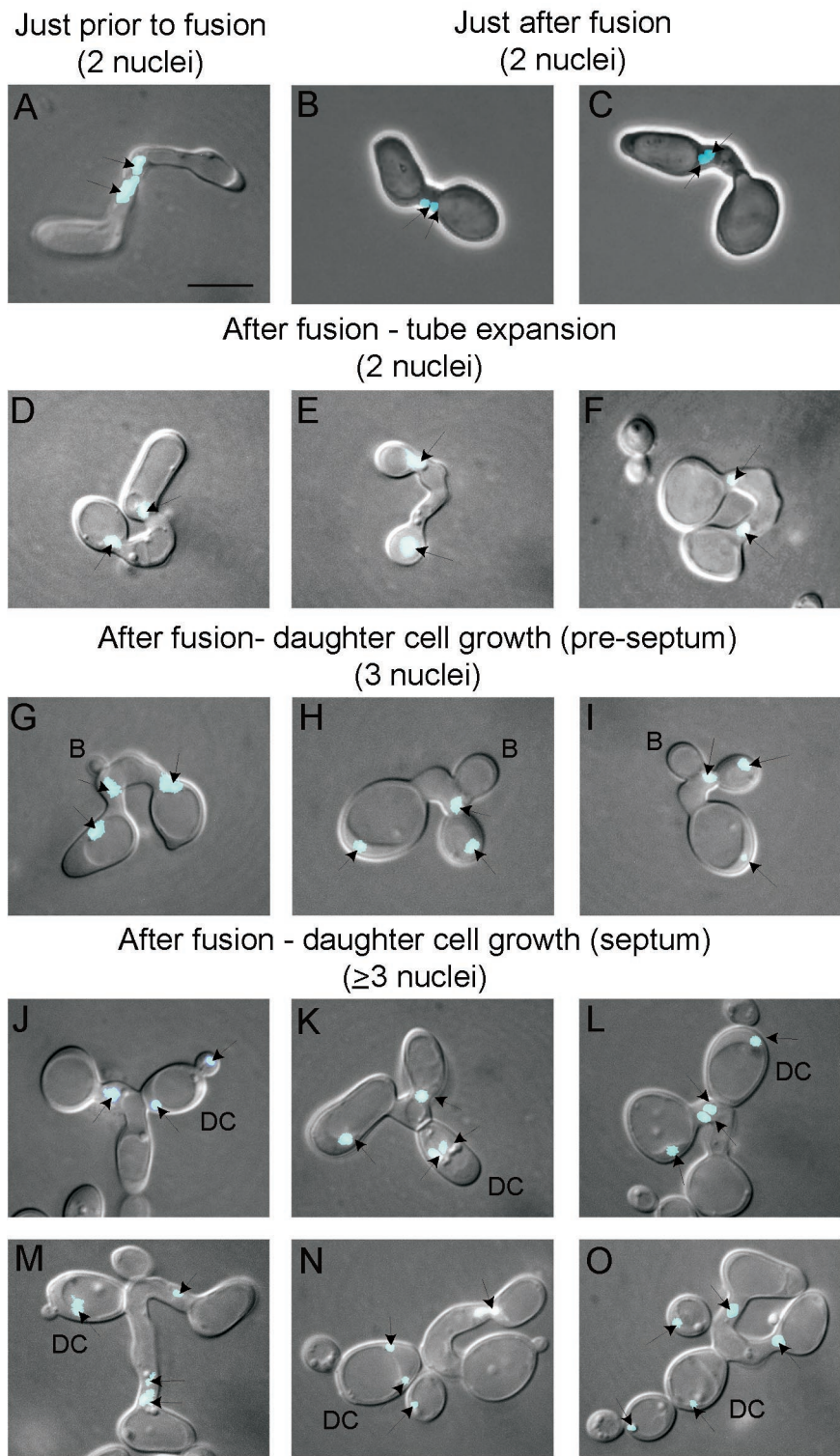After fusion - daughter cell growth (septum)
(≥3 nuclei)

FIG. 7. Nuclear configurations during the different phases of mating. Nuclei were stained with Hoechst 33342. Fluorescent images of nuclei (blue) are superimposed on DIC images. Arrows point to nuclei. B, bud; DC, daughter cell (after septation). Scale bar, 5 μm.
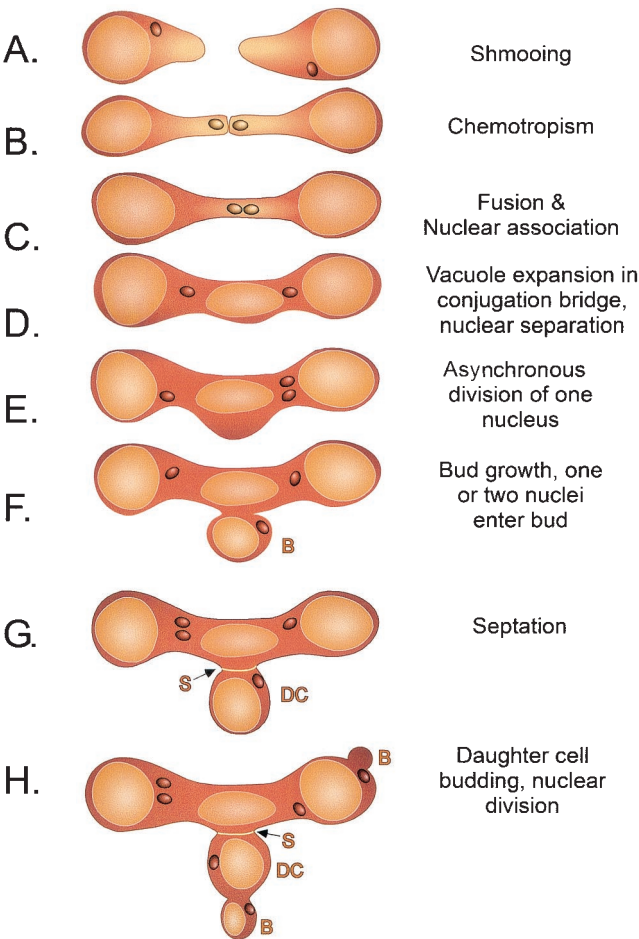
FIG. 8. Model of nuclear dynamics during zygote and daughter cell formation. The consensus sequence of events was interpreted by reviewing a number of mixed cultures of *MTL*a and *MTL*α cells. Vacuoles are light brown, and nuclei are dark brown. B, bud; S, septum; DC, daughter cell.

dium, *MTL*a and *MTL*α opaque-phase cells were mixed in modified Lee's medium, incubated until fusion, but not daughter cell growth, was maximal, and then transferred to agar containing sporulation medium (29). Crosses were performed between P37005 (*MTL*a) and 19F (*MTL*α), P37005 (*MTL*a) and WO-1 (*MTL*α), P75063 (*MTL*a) and 19F (*MTL*α), P75063 (*MTL*a) and WO-1 (*MTL*α), P75603 (*MTL*a) and P78048 (*MTL*α), 12C (*MTL*a) and WO-1 (*MTL*α), and L26 (*MTL*a) and WO-1 (*MTL*α). In every case, conjugation bridges contained multiple nuclei rather than a single fused nucleus. In the cross between L26 and WO-1, all fusion complexes (parent cells and conjugation bridges) lysed, leaving daughter cells intact. Twenty percent of the resulting daughter cells contained two or more nuclei (Fig. 10).

DISCUSSION

Here, we provide for the first time a cytological description of the mating process of *C. albicans* that had been previously detected by genetic methods (14, 20, 21). For *S. cerevisiae*, mixing *MAT*a and *MAT*α cells causes them to extend mating projections that fuse at their ends to form a connecting tube, referred to as a conjugation bridge (19). The extension of a wide, unconstricted projection, a process referred to as shmooing, is stimulated in each mating type by a pheromone released by the opposite mating type (6, 16). Nuclei arrested in G_1 by the pheromones (11) migrate into the extensions and fuse very soon after cellular fusion (5). A daughter cell then forms from the zygote. The nucleus divides, and the daughter cell receives one of the two diploid nuclei. The daughter cell then multiplies in the diploid state in rich medium. Zygote meiosis follows only when the culture is transferred to starvation medium (4). The cytological changes in mixed *MTL*a and *MTL*α cultures and the early steps in the mating process in *C. albicans* (Fig. 8) paralleled those in mixed *MAT*a and *MAT*α cultures of *S. cerevisiae*. Cells of opposite mating types extended tubes. Video analysis and 3D reconstruction revealed that tubes in close proximity grew toward each other, indicating chemotro-
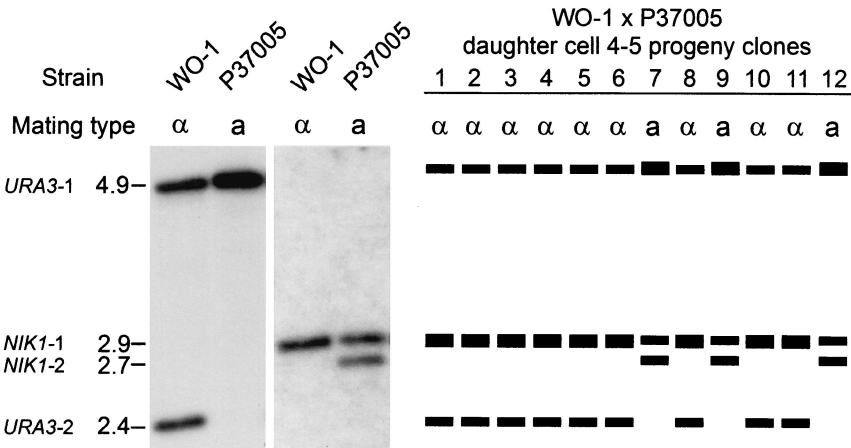

FIG. 9. Examples of Southern blot patterns of WO-1 (*MTL*α) and P37005 (*MTL*a) and progeny of a cross probed with both *URA3* and *NIK1*. (A) Southern blots. Note two *URA3* bands and one *NIK1* band for WO-1 and one *URA3* band and two *NIK1* bands for P37005. (B) Models of the banding patterns and allelism of the mating type loci of 12 progeny clones of daughter cell 4-5 (Table 3) picked from a cross between WO-1 and P37005. Note that all *MTL*α progeny exhibited the *URA3* and *NIK1* banding patterns of the *MTL*α parent strain and that all *MTL*a progeny exhibited the banding patterns of the *MTL*a parent strain. Numbers to the left of the blot are molecular sizes (in kilobases).

TABLE 3. Genotypes of the progeny of daughter cells from a cross between strains WO-1 (*MTL*α) and P37005 (*MTL***a**)[a]

Parent strain or daughter cell	Isolates	*MTL* mating type	Band			
			NIK1-1	*NIK1*-2	*URA3*-1	*URA3*-2
Strains						
P37005		**a**	+	+	+	
WO-1		α	+		+	+
Daughter cells						
3-13	1–12	**a**	+	+	+	
3-16	1–12	**a**	+	+	+	
4-6	1–12	**a**	+	+	+	
2-8	1–12	α	+		+	+
3-21	1–12	α	+		+	+
4-5	7, 9, 12	**a**	+	+	+	
	1–6, 8, 10, 11	α	+		+	+

[a] Daughter cells from fusions were picked with a micromanipulator and grown; 12 cells from each clone were in turn cloned, grown, and analyzed by Southern blot hybridization. Cells were analyzed for mating type and for the presence (+) of the two *NIK1* bands and the two *URA3* bands (Fig. 9).

pism. In many cases, tubes grew quite long and then budded apically, suggesting recovery when a tube failed to fuse to another tube extended by a cell of the opposite mating type. In the process of tube fusion, nuclei migrated from the parent cell bodies to the tube apices. Upon cellular fusion, the two nuclei were localized side by side in the conjugation bridge but there was no indication of nuclear fusion (i.e., one nucleus in the bridge). The conjugation tube formed a vacuole, which appeared to separate the nuclei to the junctions of the conjugation bridge and the original parent cell bodies. Just prior to daughter cell formation, one of the two nuclei divided. As the daughter bud grew from the conjugation tube, one or two of the nuclei entered it. After septum formation, the majority of the daughter cells contained one nucleus and a minority included two nuclei. The fusion complex of parental cells and conjugation bridge contained two to four nuclei after the septum formed between the conjugation tube and the daughter cell, suggesting that nuclear division continued in the complex.

FIG. 10. Multinucleated cells from a cross between strain L26 (*MTL***a**) and strain WO-1 (*MTL*α), of which the mixture was first incubated in modified Lee's medium until fusion occurred (but in which daughter cells did not have a chance to form) and then incubated overnight in sporulation medium. Under these conditions, 20% of the daughter cells were multinucleated. (A to C) Examples of cells with two nuclei; (D) example of a cell with four nuclei. Scale bar, 5 μm.

After the daughter cell budded and the bud matured, nuclear division resulted in one or more nuclei in the daughter cell and one nucleus in the secondary bud. This general sequence of stages (Fig. 8) was observed in crosses between strain WO-1 (*MTL*α) and either strain P37005 (*MTL***a**) or strain L26 (*MTL***a**) and between strain P78048 (*MTL*α) and strain L26 (*MTL***a**). Interestingly, the mating process generated a transient heterokaryon that was heterozygous for *MTL***a** and *MTL*α.

In both the original demonstrations of mating in vivo (14) and in vitro (20), the mating event was demonstrated by identifying cells that acquired the prototrophic markers of both the homozygous *MTL***a** strain and the homozygous *MTL*α strain. In the subsequent demonstration that the opaque-phase phenotype facilitated mating, Miller and Johnson (21) demonstrated again the acquisition of both prototrophic and genetic markers by single cells. Hull et al. (14) noted that cells that had acquired markers from both parents were mononucleate but contained more DNA than the parental cells and hence were either tetraploid or somewhere between tetraploid and diploid. Meiosis was not demonstrated. Here, we picked individual daughter cells of zygotes formed between strains WO-1 (*MTL*α) and P37005 (*MTL***a**) and tested progeny for mixing and segregation of mating types and associated genetic markers. The three marker genes resided on different chromosomes. We found that five of six individually picked daughter cells produced progeny that were exclusively *MTL***a** (Table 3) or exclusively *MTL*α and that one produced progeny that were either *MTL***a** or *MTL*α. In all six cases, the markers originally associated with *MTL***a** or with *MTL*α in the parent strains were still associated with the alternate mating types in the progeny. Hence, in the cross analysis, no segregation of markers was observed. Presumably, five of the six daughter cells received a single nucleus derived from either the *MTL***a** or *MTL*α parental cell and hence all of their progeny exhibited the genotype of one or the other parent. The sixth daughter cell that was analyzed produced progeny that were either *MTL***a** or *MTL*α, demonstrating that it had received at least one nucleus from each parent cell. These results appear to contradict the model proposed by Miller and Johnson (21), in which fusion gives rise to karyogamy and a tetraploid state. Since our results were
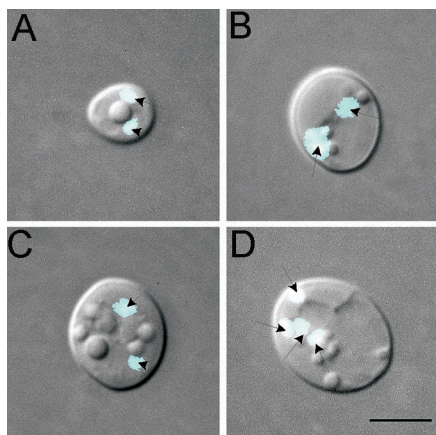
obtained from crosses between natural *MTL*-homozygous strains in the absence of selection, while those of previous studies (14, 20, 21) were obtained from crosses of engineered hemizygous strains containing auxotrophic markers, it is quite possible that tetraploidy in the latter cases was the result of selective forces. In addition, there was no indication in the previous studies that nuclear fusion occurred before daughter cell formation.

The absence of any cytological or genetic indication of nuclear fusion between natural homozygous **a** and α strains suggests heterokaryon incompatibility. Although previous studies have demonstrated the combining of selectable markers from *MTL***a** and *MTL*α strains after mixing in vivo (14) and in vitro (20, 21), no study has demonstrated subsequent segregation of markers or a reduction division, in this case from tetraploid to diploid. Our results are consistent with heterokaryon incompatibility, which is common in filamentous ascomycetes (27). In ascomycetes, incompatible strains may undergo karyogamy but the result is cell death. In our studies, fusion between *MTL***a** and *MTL*α strains did not result in nuclear fusion even though the mating process localized nuclei of opposite mating types to the center of the conjugation bridge, where fusion normally occurs in *S. cerevisiae* (5). Because progression through subsequent stages paralleled the mating process of *S. cerevisiae* and led to a viable daughter cell, heterokaryon incompatibility, as it is known from filamentous ascomycetes, cannot be an explanation for the events we have described. Since there is no obvious advantage to mating without karyogamy and recombination, aside from the exchange of the small amount of genetic information contained in the mitochondrial genome, we have entertained the possibility that if incompatibility is at play in the crosses that we have examined here, it is manifested simply by the absence of karyogamy, not by the cessation of subsequent stages in the mating process. In *S. cerevisiae*, nuclear fusion is relatively complex. Mutations in a variety of genes (*KAR1-5*, *KAR8*, *CIK1*, *CIK2*, *BIK1*, *TUB2*, *KAR71*, *SEC63*, *SEC72*, *CDC4*, *CDC28*, *CDC34*, and *CDC37*) (26) result in daughter cells with two nuclei. Dutcher and Hartwell (8, 9) have demonstrated that the products of these genes in fact prepare nuclei for fusion. It is therefore possible that such mutations have accumulated in *C. albicans*, which exhibits a primarily clonal population structure (10, 25), and that at least one strain in each of the pairs of strains tested in this study for mating carried such a mutation. Even so, it has been demonstrated with *S. cerevisiae* that in heterokaryons generated by crossing the mutant *kar1-1* strain and the wild-type *KAR1* strain, internuclear transfer of chromosomes occurs in the absence of karyogamy (7). Hence, recombination may occur in *C. albicans* without karyogamy. Alternatively, the conditions that we have used to test for mating and meiosis may have been conducive for the former but not the latter. Indeed, while rich medium supports the mating of *S. cerevisiae* cells, it does not support meiosis (4). This may not, however, be analogous to our results, since while nuclei fuse during the mating of *S. cerevisiae* cells in rich medium, they do not fuse during the mating of *C. albicans* cells. Hence, the block in rich medium for *S. cerevisiae* is at meiosis, while the block for *C. albicans* is at karyogamy. To test whether the absence of karyogamy was due to incompatibility or to the conditions in our mixing experiments, we are now in the process of performing all possible crosses between the homozygous *MTL***a** strains and the homozygous *MTL*α strains identified in a large collection of characterized clinical isolates and testing a wide variety of media and incubation conditions for cytological and genetic demonstrations of karyogamy, meiosis, and recombination.

REFERENCES

1. **Anderson, J. M., and D. R. Soll.** 1987. Unique phenotype of opaque cells in the white-opaque transition of *Candida albicans*. J. Bacteriol. **169:**5579–5588.
2. **Bedell, G. W., and D. R. Soll.** 1979. Effects of low concentrations of zinc on the growth and dimorphism of *Candida albicans*: evidence for zinc-resistant and -sensitive pathways for mycelium formation. Infect. Immun. **26:**348–354.
3. **Blignaut, E., C. Pujol, S. Lockhart, S. Joly, and D. R. Soll.** 2002. Ca3 fingerprinting of *Candida albicans* isolates from human immunodeficiency virus-positive and healthy individuals reveals a new clade in South Africa. J. Clin. Microbiol. **40:**826–836.
4. **Byers, B.** 1981. Cytology of the yeast life cycle, p. 59. *In* J. N. Strethern (ed.), The molecular biology of the yeast *Saccharomyces*: life cycle and inheritance. Cold Spring Harbor Laboratory Press, Cold Spring Harbor, N.Y.
5. **Byers, B., and L. Goetsch.** 1975. Behavior of spindles and spindle plaques in the cell cycle and conjugation in *Saccharomyces cerevisiae*. J. Bacteriol. **124:**511–523.
6. **Cross, F., L. H. Hartwell, C. Jackson, and J. B. Konopka.** 1988. Conjugation in *Saccharomyces cerevisiae*. Annu. Rev. Cell Biol. **4:**429–457.
7. **Dutcher, S. K.** 1981. Internuclear transfer of genetic information in *kar1-1/KAR1* heterokaryons in *Saccharomyces cerevisiae*. Mol. Cell. Biol. **1:**245–253.
8. **Dutcher, S. K., and L. H. Hartwell.** 1982. The role of *Saccharomyces cerevisiae* cell-division cycle genes in nuclear fusion. Genetics **100:**175–184.
9. **Dutcher, S. K., and L. H. Hartwell.** 1983. Genes that act before conjugation to prepare the *Saccharomyces cerevisiae* nucleus for caryogamy. Cell **33:**203–210.
10. **Graser, Y., M. Volovsek, J. Arrington, G. Schonian, W. Presber, T. G. Mitchell, and R. Vilgalys.** 1996. Molecular markers reveal that population structure of the human pathogen *Candida albicans* exhibits both clonality and recombination. Proc. Natl. Acad. Sci. USA **93:**12473–12477.
11. **Hartwell, L. H.** 1973. Synchronization of haploid yeast cell cycles, a prelude to conjugation. Exp. Cell Res. **76:**111–117.
12. **Heid, P. J., E. Voss, and D. R. Soll.** 2002. 3D-DIASemb: a computer-assisted system for reconstructing and motion analyzing in 4D every cell and nucleus in a developing embryo. Dev. Biol. **245:**329–347.
13. **Hull, C. M., and A. D. Johnson.** 1999. Identification of a mating type-like locus in the asexual pathogenic yeast *Candida albicans*. Science **285:**1271–1275.
14. **Hull, C. M., R. M. Raisner, and A. D. Johnson.** 2000. Evidence for mating of the "asexual" yeast *Candida albicans* in mammals. Science **289:**307–310.
15. **Lachke, S., S. Joly, K. Daniels, and D. R. Soll.** 2002. Phenotypic switching and filamentation in *Candida glabrata*. Microbiology **148:**2661–2674.
16. **Lipke, P. N., A. Taylor, and C. E. Ballou.** 1976. Morphogenetic effects of α-factor on *Saccharomyces cerevisiae* **a** cells. J. Bacteriol. **127:**610–618.
17. **Lockhart, S. R., C. Pujol, K. Daniels, M. G. Miller, A. D. Johnson, M. A. Pfaller, and D. R. Soll.** 2003. In *Candida albicans*, white-opaque switchers are homozygous for mating type. Genetics **162:**737–745.
18. **Lockhart, S. R., B. D. Reed, C. L. Pierson, and D. R. Soll.** 1996. Most frequent scenario for recurrent *Candida* vaginitis is strain maintenance with "substrain shuffling": demonstration by sequential DNA fingerprinting with probes Ca3, C1, and CARE2. J. Clin. Microbiol. **34:**767–777.
19. **MacKay, V. L., and T. R. Manney.** 1974. Mutations affecting sexual conjugation in *Saccharomyces cerevisiae*. I. Isolation and phenotypic characterization of non-mating mutants. Genetics **76:**255–271.
20. **Magee, B. B., and P. T. Magee.** 2000. Induction of mating in *Candida albicans* by construction of *MTL***a** and *MTL*alpha strains. Science **289:**310–313.
21. **Miller, M. G., and A. D. Johnson.** 2002. White-opaque switching in *Candida albicans* is controlled by the mating type (MTL) locus and allows efficient mating. Cell **110:**293–302.
22. **Mitchell, L., and D. R. Soll.** 1979. Commitment to germ tube or bud formation during release from stationary phase in *Candida albicans*. Exp. Cell Res. **120:**167–179.
23. **Pujol, C., S. Joly, S. R. Lockhart, S. Noel, M. Tibayrenc, and D. R. Soll.** 1997. Parity among the randomly amplified polymorphic DNA method, multilocus enzyme electrophoresis, and Southern blot hybridization with the moderately repetitive DNA probe Ca3 for fingerprinting *Candida albicans*. J. Clin. Microbiol. **35:**2348–2358.

24. **Pujol, C., M. Pfaller, and D. R. Soll.** 2002. Ca3 fingerprinting of *Candida albicans* bloodstream isolates from the United States, Canada, South America, and Europe reveals a European clade. J. Clin. Microbiol. **40:**2729–2740.

25. **Pujol, C., J. Reynes, F. Renaud, M. Mallie, and J. M. Bastide.** 1993. Genetic analysis of *Candida albicans* strains studied by isoenzyme electrophoresis. J. Mycol. Med. **3:**14–19.

26. **Rose, M. D.** 1996. Nuclear fusion in the yeast *Saccharomyces cerevisiae*. Annu. Rev. Cell Dev. Biol. **12:**663–695.

27. **Saupe, S. J.** 2000. Molecular genetics of heterokaryon incompatibility in filamentous ascomycetes. Microbiol. Mol. Biol. Rev. **64:**489–502.

28. **Scherer, S., and D. A. Stevens.** 1987. Application of DNA typing methods to epidemiology and taxonomy of *Candida* species. J. Clin. Microbiol. **25:**675–679.

29. **Sherman, F., G. R. Fink, and J. B. Hicks.** 1986. Laboratory course manual for methods in yeast genetics. Cold Spring Harbor Laboratory, Cold Spring Harbor, N.Y.

30. **Slutsky, B., M. Staebell, J. Anderson, L. Risen, M. Pfaller, and D. R. Soll.** 1987. "White-opaque transition": a second high-frequency switching system in *Candida albicans*. J. Bacteriol. **169:**189–197.

31. **Soll, D. R., D. Wessels, P. J. Heid, and E. Voss.** Computer-assisted reconstruction and motion analysis of the three-dimensional cell. Sci.World, in press. [Online.] http://www.thescientificworld.com.

32. **Soll, D. R., and L. Mitchell.** 1983. Filament ring formation in the dimorphic yeast *Candida albicans*. J. Cell Biol. **96:**486–493.

33. **Soll, D. R.** 1992. High-frequency switching in *Candida albicans*. Clin. Microbiol. Rev. **5:**183–203.

34. **Soll, D. R., M. Stasi, and G. Bedell.** 1978. The regulation of nuclear migration and division during pseudo-mycelium outgrowth in dimorphic yeast *Candida albicans*. Exp. Cell Res. **116:**207–215.

35. **Soll, D. R., E. Voss, O. Johnson, and D. J. Wessels.** 2000. Three-dimensional reconstruction and motion analysis of living, crawling cells. Scanning **22:**249–257.

36. **Wessels, D., E. Voss, N. Von Bergen, R. Burns, J. Stites, and D. R. Soll.** 1998. A computer-assisted system for reconstructing and interpreting the dynamic three-dimensional relationships of the outer surface, nucleus and pseudopods of crawling cells. Cell Motil. Cytoskelet. **41:**225–246.